Article

Chemistry & Biology

Growth Factor Identity Is Encoded by Discrete Coiled-Coil Rotamers in the EGFR Juxtamembrane Region

Graphical Abstract

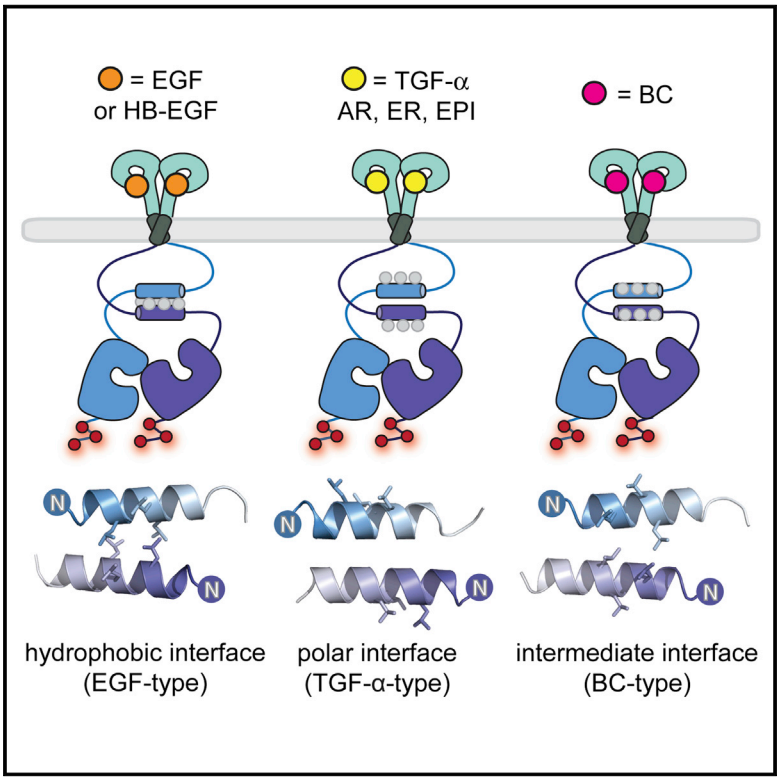

Highlights

- Three distinct, ligand-activated JM coiled-coil conformations characterized
- JM structure correlates growth factor identity with downstream signaling
- A new mechanism by which EGFR could exhibit functional selectivity is proposed
- Encoding growth factor identity in JM rotamers facilitates information transfer

Authors

Amy Doerner, Rebecca Scheck, Alanna Schepartz

Correspondence

alanna.schepartz@yale.edu

In Brief

Doerner et al. report that the EGFR juxtamembrane region assembles into three different antiparallel coiled coils whose structure both depends on growth factor identity and correlates with downstream signaling. Alternative coiled coils communicate chemical information across the plasma membrane.

Doerner et al., 2015, Chemistry & Biology 22, 776–784
June 18, 2015
http://dx.doi.org/10.1016/j.chembiol.2015.05.008

CellPress

CellPress

Chemistry & Biology
Article

Growth Factor Identity Is Encoded by Discrete Coiled-Coil Rotamers in the EGFR Juxtamembrane Region

Amy Doerner,[1] Rebecca Scheck,[1] and Alanna Schepartz[1,2,*]
[1]Department of Chemistry, Yale University, 225 Prospect Street, New Haven, CT 06520-8107, USA
[2]Department of Molecular, Cellular and Developmental Biology, Yale University, New Haven, CT 06520-8103, USA
*Correspondence: alanna.schepartz@yale.edu
http://dx.doi.org/10.1016/j.chembiol.2015.05.008

SUMMARY

Binding of transforming growth factor α (TGF-α) to the epidermal growth factor receptor (EGFR) extracellular domain is encoded through the formation of a unique antiparallel coiled coil within the juxtamembrane segment. This new coiled coil is an "inside-out" version of the coiled coil formed in the presence of epidermal growth factor (EGF). A third, intermediary coiled-coil interface is formed in the juxtamembrane region when EGFR is stimulated with betacellulin. The seven growth factors that activate EGFR in mammalian systems (EGF, TGF-α, epigen, epiregulin, betacellulin, heparin-binding EGF, and amphiregulin) fall into distinct categories in which the structure of the coiled coil induced within the juxtamembrane region correlates with cell state. The observation that coiled-coil state tracks with the downstream signaling profiles for each ligand provides evidence for growth factor functional selectivity by EGFR. Encoding growth factor identity in alternative coiled-coil rotamers provides a simple and elegant method for communicating chemical information across the plasma membrane.

INTRODUCTION

There remains an incomplete understanding of how the epidermal growth factor receptor (EGFR), the prototypic member of the receptor tyrosine kinase superfamily, communicates ligand identity across the plasma membrane. Despite multiple high-resolution views of the extracellular ligand binding (Ferguson et al., 2003; Garrett et al., 2002; Ogiso et al., 2002) and intracellular kinase (Jura et al., 2009; Zhang et al., 2006) domains and a rudimentary understanding of the basic activation mechanism (Arkhipov et al., 2013; Endres et al., 2013; Lu et al., 2010), how this information is decoded into ligand-dependent differences in cell state remains unclear (Wilson et al., 2009). In previous work, we made use of bipartite tetracysteine display (Luedtke et al., 2007) and the bis-arsenical dye ReAsH (Adams et al., 2002) to probe how ligand binding to the EGFR extracellular domain influences structure within the cytoplasmic juxtamembrane segment (JM) (Figure 1A). The JM is a short (37 amino acids) sequence that links the extracellular ligand binding and transmembrane domains to the intracellular kinase domain and stabilizes the receptor active state (Jura et al., 2009). We discovered that binding of the epidermal growth factor (EGF) to the EGFR extracellular domain induced the formation of a discrete antiparallel coiled coil (Jura et al., 2009) within the juxtamembrane-A (JM-A) segment, whereas binding of the alternative growth factor, transforming growth factor α (TGF-α), induced an alternative, helical interface whose structure was not established (Figure 1A) (Scheck et al., 2012). As predicted by nuclear Overhauser effects seen in short peptide models (Jura et al., 2009), the EGF-induced antiparallel structure is characterized by leucine residues at the *a* and *d* positions of the paired heptad repeat and complementary electrostatic interactions at positions *e* and *g* (Figure S1B). Here, we provide evidence that the helical interface formed in the presence of TGF-α is an "inside-out" version of the EGF-induced structure, in which paired polar interactions predominate at the antiparallel interface (Figure S1C). We show further that the seven growth factors that activate EGFR in mammalian systems—EGF, TGF-α, epigen (EPI), epiregulin (ER), betacellulin (BC), heparin-binding EGF (HB), and amphiregulin (AR)—fall into distinct categories in which the structure of the coiled coil induced within the JM correlates directly with cell state.

In our prior work, we designed three Cys-Cys EGFR variants (CC_H-1, -2, and -3) (Figures 1B and S1A) that reported on the formation of the EGF-induced antiparallel coiled coil in live cells (Scheck et al., 2012). When this structure forms within a receptor dimer, the assembled tetracysteine motif is poised to bind ReAsH and cause it to fluoresce. Expression of CC_H-1, -2, or -3 on the CHO-K1 cell surface resulted in a significant increase in normalized ReAsH fluorescence in the presence of EGF but not TGF-α. In contrast, expression of the EGFR variants CC_H-5 and CC_H-6 resulted in a significant increase in normalized ReAsH fluorescence in the presence of TGF-α but not EGF (Scheck et al., 2012). Given the spatial requirements for ReAsH binding (Goodman et al., 2009), these observations led to the conclusion EGFR communicates ligand identity to the cytosol through at least two, discrete, helical JM-A conformations. Here, we apply both computation and experimentation to demonstrate that the helical interface formed in the presence of TGF-α is best characterized as an "inside-out" version of the interface formed in the presence of EGF; the two antiparallel coiled coils are related by a 150° disrotatory rotation about each helix axis. We also

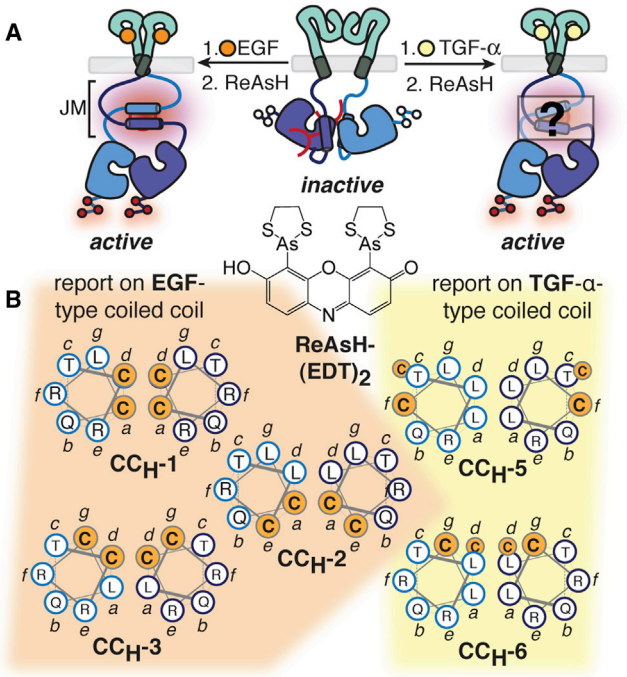

Figure 1. Probing Juxtamembrane Segment Structure within Full-Length EGFR on the Cell Surface Using Bipartite Tetracysteine Display and TIRF Microscopy

(A) EGF and TGF-α induce different structures within the EGFR juxtamembrane segment (JM) (Luedtke et al., 2007; Scheck et al., 2012; Scheck and Schepartz, 2011).

(B) Helical wheel diagrams of five EGFR variants used previously to distinguish antiparallel coiled-coil arrangements. For sequences, see Figure S1A. In CC_H-6, the Cys-Cys motifs are separated axially by a helical turn and do not assemble an ReAsH binding site (see also Figure S1).

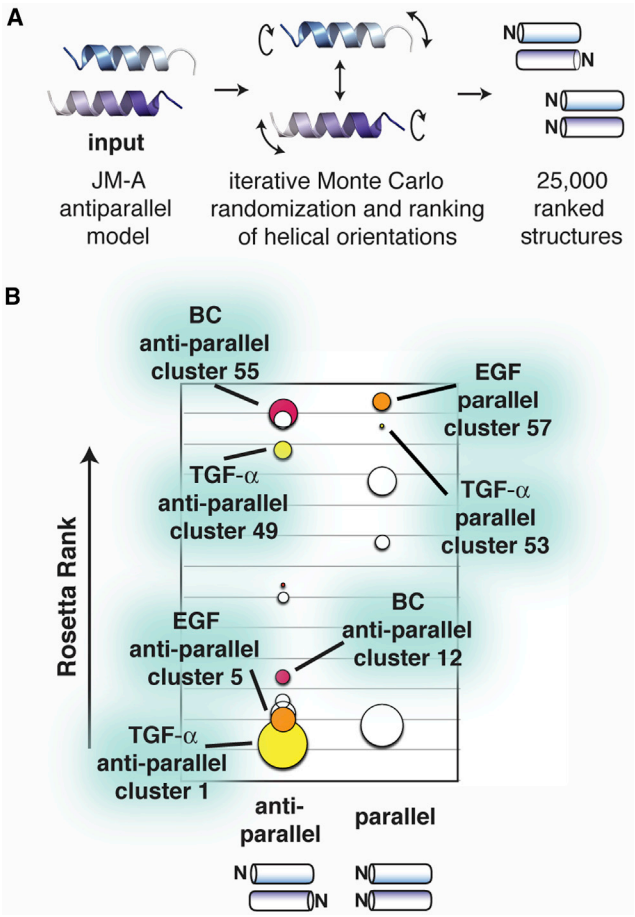

Figure 2. RosettaDock Analysis of the EGFR Juxtamembrane Segment Conformational Landscape

(A) Procedure used to generate and evaluate potential paired helix interactions of the EGFR JM.

(B) Low-energy structures identified by RosettaDock (Gray et al., 2003) ranked in order of increasing Rosetta score and separated by strand orientation. Clusters representing possible EGF-, TGF-α-, and BC-type structures are shown in orange, yellow, and pink, respectively. For the relative Rosetta rank of all clusters, see also Figure S2.

identify a third, intermediary interface formed when EGFR is stimulated with betacellulin. We show further that the seven growth factors that activate EGFR in mammalian systems (EGF, TGF-α, EPI, ER, BC, HB, and AR) fall into distinct categories in which the structure of the antiparallel coiled coil induced within the juxtamembrane segment correlates with downstream signaling outcomes. The observation that the coiled-coil state tracks with the downstream signaling profile for each ligand provides evidence for growth factor functional selectivity by EGFR. Encoding growth factor identity in alternative coiled-coil rotamers provides a simple and elegant method for communicating chemical information across the plasma membrane.

RESULTS

Evaluating the Diversity of the JM Helical Landscape In Silico

We first sought to identify the structure of the JM-A helical interface formed when EGFR is stimulated with TGF-α. Preliminary disulfide exchange and circular dichroism spectroscopy experiments revealed that peptides containing the minimal JM-A segment (residues 650–666) do not appreciably form dimers at concentrations below 150 μM (Scheck et al., 2012; Sinclair et al., 2014), precluding a straightforward biophysical analysis of the isolated peptides. Thus, we turned to an in silico analysis to explore the diversity of the JM-A conformational landscape in the absence of complicating oligomerization events, and then used bipartite tetracysteine display to detect these diverse conformations in the context of the intact receptor.

We used RosettaDock (Gray et al., 2003) to analyze thousands of potential dimeric JM-A helical interactions in silico. The interacting JM-A helices (residues 650–666) were oriented randomly, docked as rigid bodies, and the complexes subject to an all-atom minimization to optimize side-chain conformations (Figure 2A). We generated 25,000 output structures, and the top-scoring 1,000 were clustered on the basis of root-mean-square deviation (RMSD) differences. The 60 lowest-energy clusters—320 structures, roughly 1.3% of the total search space—were filtered to identify 15 clusters possessing the symmetric interface (homodimeric) that is prerequisite for ReAsH binding.

The 15 homodimeric clusters (Figure 2B) were highly diverse. As expected, the antiparallel structure for EGF-activated EGFR that was proposed by Jura et al. (2009) and confirmed by bipartite display (Scheck et al., 2012) and nuclear magnetic resonance (Endres et al., 2013; Jura et al., 2009) defined one low-energy cluster (antiparallel cluster 5) (Figure 2B and Figure S4D). However, the set of lowest-energy homodimeric clusters also contained many other structures whose helices were either parallel (36%) or antiparallel with significant deviation from cluster 5 (64%). The diversity of structures within an isolated but dimeric JM-A region predicted by RosettaDock is consistent with the short length (14 amino acids) of the interacting JM-A helices, which lack the compounding and biasing interactions provided by the intact, dimeric, receptor in complex with a specific activating growth factor. We turned to bipartite tetracysteine display to differentiate between these predicted models for full-length EGFR on the cell surface.

Evaluation of Clusters Containing Parallel Helices

We noticed that one cluster containing parallel homodimeric helices exhibited a favorable Rosetta rank (parallel cluster 57). Closer examination indicated that the structures in this cluster (Figures S3A and S3B) possessed a leucine-rich helical interface much like the EGF-induced antiparallel coil (Jura et al., 2009) observed in cells (Scheck et al., 2012). This parallel structure would have assembled a favorable tetracysteine binding site for ReAsH within the JM-A of the CC_H-1 EGFR dimer, as the Cys-Cys motif in each monomer lies near the center of the JM-A sequence (Figures S1A and S3C). As a result, CC_H-1 alone cannot distinguish between the more frequently considered antiparallel structures in cluster 5 or the parallel structures found in cluster 57. Although the Cys-Cys motifs in CC_H-2 and CC_H-3 form non-ideal ReAsH binding sites when assembled into the structures found in cluster 57, this cluster could not be ruled out without additional experimentation, as only a slight helical rotation would be required to create an ideal ReAsH binding site. Thus, we sought to determine whether the parallel helical structures in cluster 57 are populated when full-length EGFR is activated with EGF on the surface of live cells.

To identify the cluster-57 structures and distinguish them from the antiparallel structures in cluster 5, we designed a new EGFR variant suitable for bipartite tetracysteine display, CC_H-7. This variant carries a Cys-Cys motif at the N terminus of the JM-A sequence to ensure formation of a competent ReAsH binding site only if the parallel helical array in cluster 57 were to form (Figures S3E and S3F). Although CC_H-7 expressed in CHO-K1 cells is active upon treatment with EGF (Figures S3G and S3H), ReAsH treatment did not result in a significant increase in fluorescence above background (Figures S3I and S3J). The same result was observed when cells expressing CC_H-7 were treated with TGF-α. These observations failed to provide evidence for formation of the parallel coiled coil in cluster 57 when EGFR was activated with EGF (Scheck et al., 2012).

Having validated the utility of RosettaDock to refine our understanding of the EGF-induced structure within the EGFR JM-A dimer, we next sought to identify the most likely structure formed when EGFR is instead activated by TGF-α. We turned first to one set of related, parallel coiled coils (parallel cluster 53, Figures S3A and S3B) that would support ReAsH binding by the two previously reported EGFR variants CC_H-5 and CC_H-6 (Figures 1B and S3D), and thus could represent the alternative TGF-α-induced conformation(s). To test for this parallel structure using bipartite tetracysteine display, we designed EGFR variant CC_H-8, using the same strategy used to design CC_H-7, with cysteine residues at the C terminus of the helical interaction (Figures S3E and S3F). As was found for experiments employing CC_H-7, while CC_H-8 expressed in CHO-K1 cells is active upon treatment with TGF-α (Figures S3G and S3H), treatment with ReAsH led to no significant increase in fluorescence above background (Figures S3I and S3J). Taken together, the in silico and bipartite display experiments suggest that neither EGF nor TGF-α induce the formation of a parallel helical interface within activated EGFR.

Evaluation of Clusters Containing Antiparallel Helices

Having ruled out the parallel structure clusters, we next considered the large number of low-energy antiparallel structure clusters identified by RosettaDock to determine whether any could be populated when EGFR is activated with TGF-α. We focused on two clusters whose antiparallel structures were both low energy and compatible with the previously observed ReAsH binding to EGFR variants CC_H-5 and/or CC_H-6 upon TGF-α activation (Figures 1B and S1A): clusters 1 and 49 (Figures 2B, 3A, and S4D) (Scheck et al., 2012). Antiparallel cluster 1 contains lower-energy structures, but the structures in antiparallel cluster 49 form better ReAsH binding sites with the CC_H-5 and CC_H-6 Cys-Cys motifs (Figure S4A). We thus turned to bipartite tetracysteine display to differentiate between these models for TGF-α-activated EGFR expressed on the mammalian cell surface.

Differentiating between the structures in clusters 1 and 49 using ReAsH and bipartite tetracysteine display required careful design. This design recognizes that ReAsH binding sites on antiparallel coiled coils fall into three categories (Figure 4). Antiparallel arrays with Cys-Cys motifs at positions *a* and *d*, *g* and *d*, or *a* and *e* within a single heptad repeat (shown in green) support robust ReAsH binding and fluorescence, whereas those with Cys-Cys motifs at positions *f* and *c* and *f* and *b* (shown in red) do not. More context dependent are sites in the third category, antiparallel arrays carrying Cys-Cys motifs at positions *b* and *e* or *c* and *g* (shown in gray): these structures could support ReAsH binding and fluorescence in the context of a flexible JM structure. With these guidelines, we designed CC_H-9 to differentiate between the structures in clusters 1 and 49 (Figure 3B). In this EGFR variant, the Cys-Cys motif occupies the favorable *g* and *d* (and *g′* and *d′*) positions if the helices are arranged as prescribed by cluster 1, and the unfavorable *f* and *c* (and *f′* and *c′*) positions if the helices are arranged as prescribed by cluster 49 (Figure S4B). Thus, TGF-α-treated cells expressing CC_H-9 should fluoresce after ReAsH treatment if a cluster-1 coiled coil is formed within the EGFR JM-A, but not if a cluster-49 coiled coil has formed.

Evidence that the TGF-α-Induced Coiled Coil Is Inside-Out

Examination of cells transfected with CC_H-9 (Figure 3C) revealed that addition of TGF-α led to a greater than 2-fold increase in ReAsH fluorescence in comparison with untreated CC_H-9-expressing cells, favoring cluster 1 as the JM-A structure formed

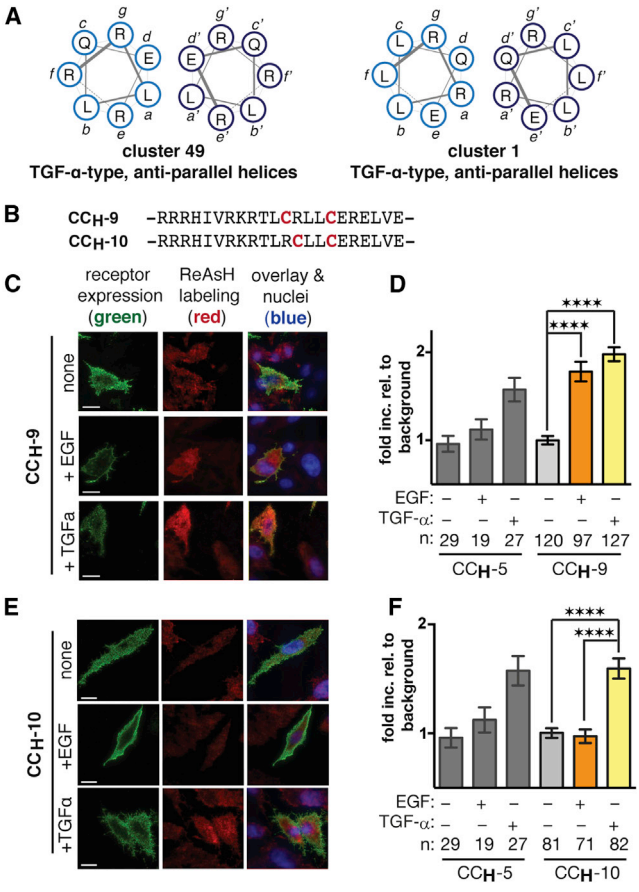

Figure 3. TGF-α Induces an "Inside-Out" Helical Interaction in the JM-A

(A) Helical wheel diagrams illustrating two antiparallel interfaces potentially adopted in the presence of TGF-α.

(B) JM-A regions of CC_H-9 and CC_H-10.

(C and E) TIRF images of CHO-K1 cells expressing either FLAG-tagged CC_H-9 or CC_H-10 (green fluorescence) and treated with EGF or TGF-α (1 ng/ml) and ReAsH. Scale bars represent 10 μm.

(D and F) Quantified fold increase in expression-corrected ReAsH fluorescence over background of cells expressing CC_H-9 or CC_H-10 and treated with or without EGF or TGF-α. We attribute the slightly lower ReAsH fluorescence of CC_H-10 to the lower activity of this mutant (see also Figure S4E). Error bars represent SE. ****$p < 0.0001$ from one-way ANOVA with Bonferroni post-test (see also Figure S4).

in the presence of TGF-α and ruling out cluster 49 (Figure 3D). Nevertheless, we observed that cells transfected with CC_H-9 also exhibited a 1.5-fold increase in ReAsH fluorescence in the presence of EGF, presumably because when the EGF-type coiled coil is formed (cluster 5), the Cys-Cys motif in CC_H-9 occupies the ambiguous *b* and *e* positions (Figure S4B). As we desired an EGFR variant that would bind ReAsH and fluoresce only when activated with TGF-α, we next designed CC_H-10 (Figure 3B). Here, the Cys-Cys motif occupies the favorable *a* and *d* (and *a′* and *d′*) positions if the helices are arranged as prescribed by cluster 1 (induced by TGF-α) and the unfavorable *b* and *f* (and *b′* and *f′*) positions if the helices are arranged as prescribed by cluster 5 (induced by EGF) (Figure S4C). As a result, we would expect that cells expressing CC_H-10 should fluoresce after ReAsH treatment when a cluster-1 structure is present, but not when a cluster-5 coiled coil has formed; therefore, these cells should fluoresce only in the presence of TGF-α. Western blot analysis of cells transfected with CC_H-10, WT EGFR and CC_H-1 showed similar patterns of C-terminal phosphorylation (Figures S4E and S4F); total internal reflection fluorescence (TIRF) microscopy (Figure 3E) revealed that addition of TGF-α to cells transfected with CC_H-10 led to a 1.5-fold increase in ReAsH fluorescence, whereas addition of EGF had no effect (Figure 3F). Taken together, the observation of robust ReAsH fluorescence when cells expressing either CC_H-9 or CC_H-10 are treated with TGF-α provides compelling evidence that the antiparallel helical structures in cluster 1 best represent the JM when EGFR is activated by TGF-α. Moreover, the EGFR variant CC_H-10 can specifically detect this conformation and distinguish it from the EGF-activated state embodied by cluster 5.

Coiled-Coil Structure Correlates with Effect on Cell State

Seven growth factors activate EGFR, five in addition to EGF and TGF-α: EPI, ER, BC, AB, and AR. Numerous studies have shown that these seven growth factors segregate into two categories when their effects on downstream signaling are compared: activation with EGF, HB, or BC leads to greater receptor down-regulation and a shorter signaling pulse, whereas activation with TGF-α, AR, ER, or EPI promote receptor recycling and sustained signaling that increases cell proliferation (Baldys et al., 2009; Ebner and Derynck, 1991; Reddy et al., 1998; Roepstorff et al., 2009; Seth et al., 1999; Thoresen et al., 1998; Wilson et al., 2012). As ligand identity must be translated through the receptor to intracellular signaling proteins, we sought to determine, using CC_H-1 and CC_H-10, whether these signaling differences correlated with JM-A conformation. To evaluate the presence of the EGF-type coiled coil (represented by cluster 5) or the TGF-α-type coiled coil (represented by cluster 1), we treated cells expressing the EGFR variants CC_H-1 or CC_H-10 with saturating concentrations (as determined by western blot, see Figures S5A and S5H) of AR, BC, ER, EPI, and HB, and monitored ReAsH fluorescence (Figures 5A and S5B). Examination of cells transfected with CC_H-1 revealed a 2-fold increase in ReAsH fluorescence upon addition of BC, HB, and EGF, but not upon addition of TGF-α, AR, ER, or EPI. By contrast, cells transfected with CC_H-10 displayed a 1.5-fold increase in ReAsH fluorescence upon addition of TGF-α, AR, and ER and a 1.3-fold increase for BC and EPI, but no increase in ReAsH fluorescence was observed upon addition of HB and EGF (Figure 5A). We attribute the lower fold increase upon EPI treatment to lower ligand potency, as detected by EGFR autophosphorylation (Figures S5A and S5H). Thus, with the exception of BC (vide infra), there is a direct correlation between the effect of a growth factor on JM-A structure and the temporal dynamics of the overall signaling response.

A Third JM Conformation Is Formed upon BC Activation

Among the growth factors that activate EGFR, BC is unique in its ability to elicit robust ReAsH fluorescence from cells expressing either CC_H-1 or CC_H-10 (Figure 5A). This observation suggests that BC either induces both the TGF-α- and EGF-type coiled coils, presumably due to a significant increase in flexibility, or

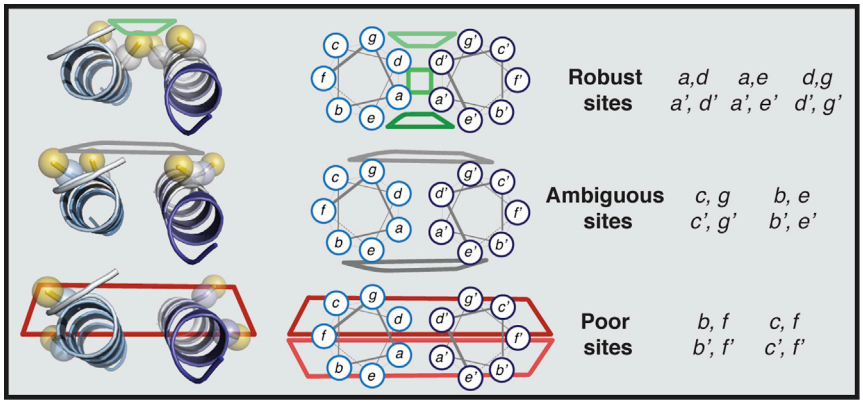

Figure 4. Categorization of Three Types of Cys-Cys ReAsH Binding Sites Formed by Dimeric Coiled Coils as Defined by Cysteine Proximity

that it induces a third, intermediary conformation that is compatible with ReAsH binding by both CC_H-1 and CC_H-10. To distinguish these possibilities, we returned to the top-scoring structure clusters predicted by RosettaDock (Figure 2B). Because BC activation led to robust ReAsH fluorescence in both CC_H-1 and CC_H-10-expressing cells, we looked to identify structures that positioned the Cys-Cys motifs in both CC_H-1 and CC_H-10 such that ReAsH fluorescence could be observed using either variant (Figure 4). This strategy identified three possible models: those in clusters 12, 55, and 49 (Figures 5B and S5E) (see Figure S5C for Cys-Cys motif placements in each model).

To differentiate between these three models, we turned to previously designed EGFR variants. First, we predicted that CC_H-9 should provide a robust ReAsH binding site if the JM-A were to assemble into structures in cluster 12 or 55, but a poor site if it assembled into structures from cluster 49 (Figure S5D). Treatment of CC_H-9-expressing cells with BC led to a 2-fold increase in ReAsH fluorescence relative to untreated cells (Figures 5D and S5G). The increase in ReAsH fluorescence observed in this case effectively rules out the formation of cluster-49 structures in the presence of BC, but fails to differentiate between the structures represented by clusters 12 and 55. Thus, we turned to CC_H-5, which would generate a poor ReAsH binding site if the JM-A is assembled as prescribed by cluster 12, and an ambiguous site if assembled as prescribed by cluster 55. Treatment of CC_H-5-expressing cells with BC did not result in a significant increase in ReAsH fluorescence relative to untreated cells (Figures 5D and S5G). The fact that CC_H-5 does not bind ReAsH upon activation by BC supports the model represented by cluster 12, which was predicted to display a poor site for ReAsH binding with the CC_H-5 Cys-Cys motifs (Figure S5D). Together, these results suggest that activation by BC does not simply increase the flexibility of the JM-A, but rather leads to the formation of a discrete helical interface that is represented by the structures in cluster 12.

DISCUSSION

The TGF-α-type antiparallel coiled coil induced in the JM-A by TGF-α, AR, EPI, and ER and identified by tetracysteine bipartite display differs in unmistakable ways from the EGF-type structure identified previously (Figure 5E) (Jura et al., 2009). With TGF-α bound, the two JM-A helices are rotated by 150° in opposite directions about the helical axis relative to the EGF-bound structure. This disrotatory motion flips the coiled coil inside-out, effectively interchanging those residues at the coiled-coil interface for those on the outside surface. In contrast to the coiled-coil interface induced by EGF, which is stabilized by leucines at the *a* and *d* positions and complementary salt bridge interactions at positions *e* and *g*, the TGF-α-type interface contains polar residues at these positions and leucine residues on the coiled-coil exterior (Figures S1B and S1C). In particular, our data point to a TGF-α-induced antiparallel structure stabilized by salt bridge/polar interactions between R657 (at position *a*) and R656 (at position *g*) on one helix and E′661 (at position *e*′) and Q′660 (at position *d*′), respectively, on the other. The JM-A conformation induced when EGFR is activated by BC, represented by cluster 12, is intermediate between the EGF- and TGF-α-activated structures, possessing both a hydrophobic and polar interface. Specifically, the BC-type coiled coil utilizes a leucine interface at the *d* and *g* (and *d*′ and *g*′) positions while using complementary polar interactions between R656 and Q660 at the *a* and *e* (and *a*′ and *e*′) positions. It has been hypothesized that the residues on the outside of the short coiled coil could interact with the membrane (Endres et al., 2013; Jura et al., 2009). While we chose to examine the unbiased interaction between the two JM-A helices, we did observe positively charged residues on the outside of the EGF-activated (R653 and R657), TGF-α-activated (K652 and R662), and BC-activated (R651, R657, and R662) conformations, further validating these models in the context of the whole, membrane-embedded receptor.

We note that while coiled-coil interfaces in natural proteins are often stabilized by hydrophobic interactions, there has been a more recent appreciation of stabilizing polar salt bridges (Meier et al., 2010). In fact, among dimeric, antiparallel polar coiled-coil interfaces, the most common interfacial motif consists of polar residues at the core positions *gd*′, *dg*′, *ae*′, and *ea*′: precisely the arrangement seen in TGF-α-cluster 1 (Meier et al., 2010). Coiled coils stabilized by polar interactions have been observed in proteins whose function demands multiple interhelical interfaces (Croasdale et al., 2011) and short sequences that facilitate dimerization (Burkhard et al., 2000), two characteristics shared with the EGFR JM. Thus, the JM-A sequence, which possesses residues for both a hydrophobic helical interface and multiple salt bridging residues, uniquely allows the receptor to adopt multiple, distinct conformations.

In this work, we correlate previously identified ligand-dictated, downstream signaling differences to induced structure within the JM: a more down-regulated, shorter signaling pulse upon EGF and HB-EGF activation is associated with formation of a JM-A conformation in which leucine residues mediate the interhelical

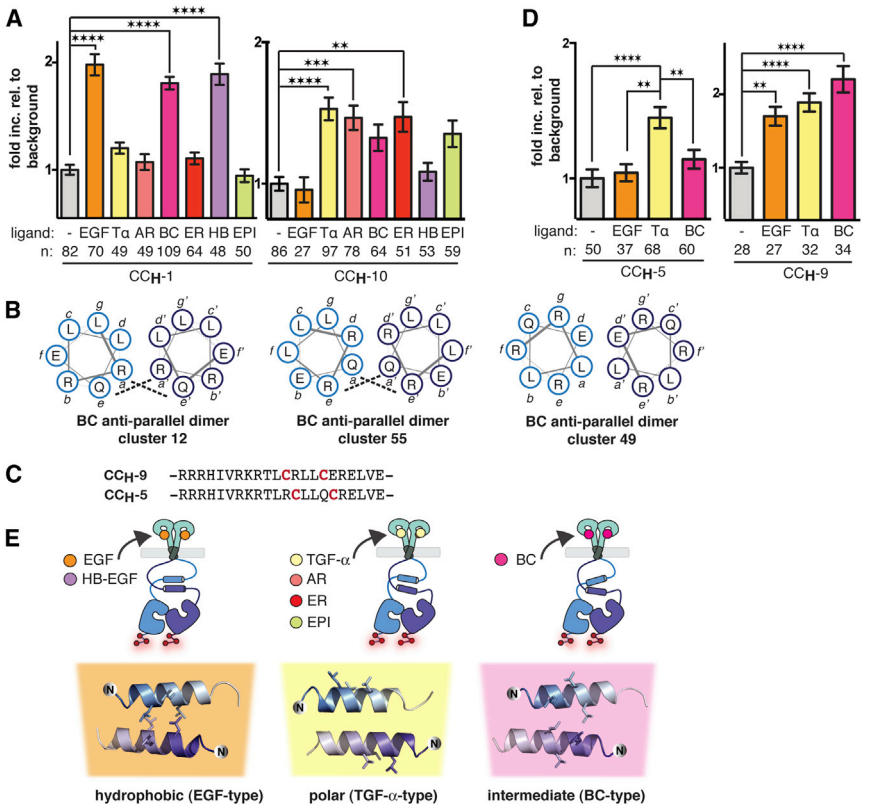

Figure 5. JM-A Conformation Correlates with Effects on Downstream Signaling

(A) Quantified fold increase in expression-corrected ReAsH fluorescence over background of cells expressing CC_H-1 or CC_H-10 and treated with either EGF, TGF-α, BC, HB-EGF (1 ng/ml) or AR, ER, or EPI (2 μg/ml). For TIRF microscopy images and western blots showing the activity of CC_H-1 and CC_H-10 upon stimulation with each growth factor, see also Figures S5A and S5B.

(B) Helical wheel diagrams illustrating the interfaces of three antiparallel structures potentially adopted in the BC-activated JM-A region of EGFR.

(C) CC_H-5 and CC_H-9 primary sequences.

(D) Quantified fold increase in expression-corrected ReAsH fluorescence over background of cells expressing CC_H-5 or CC_H-9 and treated with or without EGF, TGF-α, or BC (1 ng/ml). For helical wheel diagrams showing the relative orientation of Cys-Cys motifs in EGFR variants when assembled into the antiparallel coiled coils defined by clusters 12, 55, and 49, see Figures S5C and S5D. For TIRF microscopy images and western blots showing the activity of CC_H-5 and CC_H-9 upon stimulation with EGF, TGF-α, and BC, see Figures S5F and S5G.

(E) EGFR stimulates three ligand-stimulated JM-A conformations. Activation by EGF and HB-EGF is best represented by cluster-5 structures with a hydrophobic interface while activation by TGF-α, AR, ER, and EPI are best represented by cluster-1 structures with a polar interface. BC-activated EGFR likely adopts an intermediary conformation represented by cluster 12. All structures show the side chains of L655, L658, and L659 explicitly. Error bars represent SE. $^{**}p < 0.01$, $^{***}p < 0.001$, $^{****}p < 0.0001$ from one-way ANOVA with Bonferroni post-test (see also Figure S5).

interface. On the other hand, the more recycled receptor with a sustained signaling pulse that results from TGF-α, AR, ER, and EPI activation is associated with formation of an inside-out JM-A conformation in which polar interactions line the interface and hydrophobic leucine residues are on the outside. The correlation breaks down for a single outlier, BC, whose activated JM-A conformation is intermediary with only a 50° disrotatory motion separating the two. It is possible that these two structures are close enough to induce similar signaling downstream of the receptor, or perhaps the difference in helical structure has an impact on signaling outcomes that are presently not appreciated (Saito et al., 2004). It has been posited that receptor flexibility is an intrinsic property of receptors capable of engaging multiple ligands and signaling proteins (Nygaard et al., 2013), potentially explaining why this molecular mechanism has been difficult to study in many receptor tyrosine kinases.

The ligand-dependent differences in JM structure uncovered in this work imply analogous ligand-dependent differences in the conformation of the bound ECD that are propagated to the JM through domain IV and the transmembrane domain. We have previously shown that differences in the binding modes of EGF and TGF-α must lead to differential positioning of domain IV in the ECD (Scheck et al., 2012). In addition, molecular dynamics simulations have revealed subtle differences in the ligand-bound conformations of the ECD (Sanders et al., 2013), and domain II has recently been identified as a potential mediator of subtle differences in ligand binding and specific receptor states (Bessman et al., 2014). Furthermore, mutations in the JM-A region alter the energetics of ligand binding to the ECD (Macdonald-Obermann and Pike, 2009), and there is clear evidence that the active conformation of the EGFR transmembrane is flexible and capable of adopting multiple conformations (Endres et al., 2013), like other single-pass transmembrane domains (Dominguez et al., 2014). Taken together, these observations support a model in which different ligand-dependent JM-A conformations result from three distinct ligand-bound ECD conformations that are transmitted faithfully through the membrane-sequestered transmembrane helical dimer.

Our results support a recent theory that EGFR displays ligand functional selectivity (Wilson et al., 2009), or biased signaling, such that activation by a ligand stimulates the population of distinct conformations that singularly dictate downstream signaling differences (Kahsai et al., 2011; Liu et al., 2012). While many RTKs respond to multiple ligands and effect ligand-dependent signaling, a molecular link between the structure of the ligand-bound receptor and its distinct ligand-mediated cellular outcome has not been firmly established (Thomas et al., 2011). Here, we report direct evidence that different extracellular EGFR ligands induce distinct conformations of the intracellular JM-A region of the receptor. There are multiple mechanisms by which different JM conformations could dictate downstream signaling. First, it is possible that proteins known to bind to the JM-A region and induce various signaling pathways, such as calmodulin (Martin-Nieto and Villalobo, 1998), Nck adaptor

protein (Hake et al., 2008), $G\alpha_S$ (Poppleton et al., 2000), PKC (Hunter et al., 1984), and $p38^{MAPK}$ (Takishima et al., 1988), are preferentially recruited by one specific JM conformation. It is also possible that differential display of nuclear (Lin et al., 2001) and basolateral (Ryan et al., 2010) sorting motifs in the JM-A could differentially traffic the receptor. Lastly, specific JM-A conformations could directly bind to the surface of the asymmetric kinase dimer, leading to further propagation of subtle conformational changes through the kinase domains and differential C-terminal tail phosphorylation (Wilson et al., 2009). It may be possible to generate EGFR mutants that assemble into one coiled coil or the other, irrespective of growth factor treatment. These mutants will provide confirmation that both structures are capable of autophosphorylation and evaluate the role of each in downstream events. Our observation of distinct ligand-dependent JM-A conformations in surface receptors does not support the current belief that ligand-dependent downstream signaling differences result from differences in the pH-dependent ligand occupancy of endocytosed receptors, as our experiments were conducted with endocytosis inhibited (Ebner and Derynck, 1991; French et al., 1995). Interestingly, the validity of this theory has also been questioned by others (Fortian and Sorkin, 2014), and it is possible that ligand-dependent effects on cell state arise from a more complicated mechanism. Further experiments are necessary to distinguish between these various theories.

SIGNIFICANCE

Many common cancers are caused by aberrant activation of the EGFR. How EGFR is activated by growth factors to direct different signaling outcomes is not understood. While it was originally proposed that growth factor-dependent signaling differences arise from differential occupancy of the receptor during endocytosis, here we show that EGFR decodes growth factor identity by adopting discrete conformations in each ligand-activated state. We use a pro-fluorescent small molecule probe in combination with computational modeling to detect and characterize three distinct ligand-activated conformations. We further discover that these conformations track with the downstream signaling profiles for each ligand, providing evidence for growth factor functional selectivity by EGFR.

EXPERIMENTAL PROCEDURES

RosettaDock Modeling of JM Interfaces

RosettaDock (Rosetta 3.4) (Gray et al., 2003) was used for all docking calculations. We used the JM model described by Jura et al. (2009) as the input, with each helix of the short coiled-coiled-like structure treated as one of the two docking partners. This structure was run first through the docking prepack algorithm (Rosetta 3.4) to optimize initial side-chain positions. The initial, relative positions of the two helices were both randomized. Both the outer and inner stages of the low-resolution step of the docking procedure were cycled 20 times and all possible side-chain rotamers were incorporated into the algorithm for the high-resolution step. 25,000 output structures were created and sorted based on overall RosettaDock energy score. The 1,000 top-scoring structures were then processed by the cluster application (Rosetta 3.4) whereby the total number of clusters was limited to 100 and a 1.4-Å RMSD cutoff was used. The resulting clusters were ranked on the basis of their Rosetta energy scores.

ReAsH Labeling Assay

ReAsH labeling was accomplished as described previously (Scheck et al., 2012) with the following changes: 63,000 cells were used to seed the experiment, Disperse Blue was omitted from the ReAsH labeling step, a 1:2,000 dilution of Alexa Fluor 488 Goat Antimouse IgG, IgA, IgM (H + L) Antibody (2 mg/ml) was used as the secondary antibody in the last step, and nuclei were labeled with 1.62 μM Hoechst 33342 for 5 min at 37°C. Additionally, EGF, TGF-α, HB-EGF, and BC were used at a concentration of 100 ng/ml while ligands with a weaker affinity including AR, ER, and EPI were used at concentration of 2 μg/ml.

TIRF Microscopy

TIRF microscopy was conducted on a Leica microsystems AM TIRF MC DMI6000B fitted with an EM-CCD camera (Hamamatsu) with either the HCX PL APO 63×/1.47 or 100×/1.47 oil corrective objectives. A 12-V 100-W halogen lamp was used for fluorescence application. In TIRF mode, EGFR labeled with Alexa Fluor 488 was excited using the 488-nm laser and ReAsH was excited with the 561-nm laser, while signals were processed in the QAD TIRF filtercube. Hoechst-stained nuclei were visualized in epifluorescence mode with the cyan fluorescent protein filtercube. Images were analyzed as described previously (Scheck et al., 2012).

Western Blot Analysis of EGFR Autophosphorylation

CHO-K1 cells were maintained in Ham's F-12K (Kaighn's) medium with 10% fetal bovine serum at 37°C with 5% CO_2. 100-mm dishes were seeded with 1.5×10^6 cells for 18 hr, at which point the cells were transfected with either wild-type or Cys-Cys EGFR variants of EGFR with TransIT-CHO kit according to the manufacturer's instructions. After 8 hr, the cells were serum starved for another 18 hr and then harvested using non-enzymatic cell dissociation solution and washed with Dulbecco's PBS, and 500,000 cells were pipetted into wells of a 96-well plate. To each well was added a 200-μl aliquot of one of the following reagents, and the incubation continued at 37°C for 5 min: serum-free media, 100 ng/ml of EGF, TGF-α, HB-EGF, or BC in serum-free media, or 2 μg/ml of AR, ER, or EPI in serum-free media. Cells were then washed with serum-free media and lysed in 120 μl of 50 mM Tris, 150 mM NaCl, 1 mM EDTA, 1 mM NaF, and 1% Triton X-100 (pH 7.5) with protease and phosphatase inhibitors (1 tablet/10 ml) for 1–2 hr on ice. Lysate was then clarified at 14,000 rcf for 25 min at 4°C. For western blot analysis, lysates were run on a 10% polyacrylamide SDS-PAGE gel and transferred to polyvinylidene fluoride membranes using an iBlot (Invitrogen). Membranes were blocked with 5% milk in TBS-T (50 mM Tris, 150 mM NaCl, 0.1% Tween, pH 7.4) for 1–3 hr followed by an overnight incubation at 4°C of either rabbit α-pY1173 or mouse α-FLAG primary antibodies. Blots were then washed with 5% milk in TBS-T and incubated with either α-rabbit or α-mouse horseradish peroxidase conjugate secondary antibodies for 1 hr at room temperature, then washed with TBS-T and visualized using Clarity Western ECL reagents.

Statistical Analysis

Comparisons within groups were made using ANOVA. Pairwise comparisons within groups were made using Bonferroni's post-test after finding a significant difference using ANOVA. The p values are corrected using Bonferroni's method (Shaffer, 1995) so that the family-wise error rate is 0.05.

SUPPLEMENTAL INFORMATION

Supplemental Information includes Supplemental Experimental Procedures and five figures and can be found with this article online at http://dx.doi.org/10.1016/j.chembiol.2015.05.008.

AUTHOR CONTRIBUTIONS

A.D., R.S., and A.S. designed research; A.D. and R.S. performed research; A.D., R.S., and A.S. analyzed data; A.D., R.S., and A.S. wrote the paper.

ACKNOWLEDGMENTS

The authors are grateful to the N.I.H. (GM 83257 to A.S. and F32 GM087092 to R.A.S.) for support of this research. A.D. was supported by an NIH Training Grant in Biophysics (5T32GM008283-28).

Received: April 3, 2015
Revised: May 4, 2015
Accepted: May 13, 2015
Published: June 18, 2015

REFERENCES

Adams, S., Campbell, R., Gross, L., Martin, B., Walkup, G., Yao, Y., Llopis, J., and Tsien, R. (2002). New biarsenical ligands and tetracysteine motifs for protein labeling in vitro and in vivo: synthesis and biological applications. J. Am. Chem. Soc. *124*, 6063–6076.

Arkhipov, A., Shan, Y., Das, R., Endres, N.F., Eastwood, M.P., Wemmer, D.E., Kuriyan, J., and Shaw, D.E. (2013). Architecture and membrane interactions of the EGF receptor. Cell *152*, 557–569.

Baldys, A., Gooz, M., Morinelli, T.A., Lee, M.H., Raymond, J.R., Luttrell, L.M., and Raymond, J.R. (2009). Essential role of c-Cbl in amphiregulin-induced recycling and signaling of the endogenous epidermal growth factor receptor. Biochemistry *48*, 1462–1473.

Bessman, N.J., Bagchi, A., Ferguson, K.M., and Lemmon, M.A. (2014). Complex relationship between ligand binding and dimerization in the epidermal growth factor receptor. Cell Rep. *9*, 1306–1317.

Burkhard, P., Kammerer, R.A., Steinmetz, M.O., Bourenkov, G.P., and Aebi, U. (2000). The coiled-coil trigger site of the rod domain of cortexillin I unveils a distinct network of interhelical and intrahelical salt bridges. Structure *8*, 223–230.

Croasdale, R., Ivins, F.J., Muskett, F., Daviter, T., Scott, D.J., Hardy, T., Smerdon, S.J., Fry, A.M., and Pfuhl, M. (2011). An undecided coiled coil: the leucine zipper of Nek2 kinase exhibits atypical conformational exchange dynamics. J. Biol. Chem. *286*, 27537–27547.

Dominguez, L., Foster, L., Meredith, S.C., Straub, J.E., and Thirumalai, D. (2014). Structural heterogeneity in transmembrane amyloid precursor protein homodimer is a consequence of environmental selection. J. Am. Chem. Soc. *136*, 9619–9626.

Ebner, R., and Derynck, R. (1991). Epidermal growth-factor and transforming growth factor-alpha - differential intracellular routing and processing of ligand-receptor complexes. Cell Regul. *2*, 599–612.

Endres, N.F., Das, R., Smith, A.W., Arkhipov, A., Kovacs, E., Huang, Y.J., Pelton, J.G., Shan, Y.B., Shaw, D.E., Wemmer, D.E., et al. (2013). Conformational coupling across the plasma membrane in activation of the EGF receptor. Cell *152*, 543–556.

Ferguson, K.M., Berger, M.B., Mendrola, J.M., Cho, H.-S., Leahy, D.J., and Lemmon, M.A. (2003). EGF activates its receptor by removing interactions that autoinhibit ectodomain dimerization. Mol. Cell *11*, 507–517.

Fortian, A., and Sorkin, A. (2014). Live-cell fluorescence imaging reveals high stoichiometry of Grb2 binding to the EGF receptor sustained during endocytosis. J. Cell Sci. *127*, 432–444.

French, A.R., Tadaki, D.K., Niyogi, S.K., and Lauffenburger, D.A. (1995). Intracellular trafficking of epidermal growth-factor family ligands is directly influenced by the Ph sensitivity of the receptor-ligand interaction. J. Biol. Chem. *270*, 4334–4340.

Garrett, T.P.J., McKern, N.M., Lou, M.Z., Elleman, T.C., Adams, T.E., Lovrecz, G.O., Zhu, H.J., Walker, F., Frenkel, M.J., Hoyne, P.A., et al. (2002). Crystal structure of a truncated epidermal growth factor receptor extracellular domain bound to transforming growth factor alpha. Cell *110*, 763–773.

Goodman, J.L., Fried, D.B., and Schepartz, A. (2009). Bipartite tetracysteine display requires site flexibility for ReAsH coordination. Chembiochem *10*, 1644–1647.

Gray, J.J., Moughon, S., Wang, C., Schueler-Furman, O., Kuhlman, B., Rohl, C.A., and Baker, D. (2003). Protein-protein docking with simultaneous optimization of rigid-body displacement and side-chain conformations. J. Mol. Biol. *331*, 281–299.

Hake, M.J., Choowongkomon, K., Kostenko, O., Carlin, C.R., and Sonnichsen, F.D. (2008). Specificity determinants of a novel Nck interaction with the juxtamembrane domain of the epidermal growth factor receptor. Biochemistry *47*, 3096–3108.

Hunter, T., Ling, N., and Cooper, J.A. (1984). Protein kinase-C phosphorylation of the EGF receptor at a threonine residue close to the cytoplasmic face of the plasma-membrane. Nature *311*, 480–483.

Jura, N., Endres, N.F., Engel, K., Deindl, S., Das, R., Lamers, M.H., Wemmer, D.E., Zhang, X.W., and Kuriyan, J. (2009). Mechanism for activation of the EGF receptor catalytic domain by the juxtamembrane segment. Cell *137*, 1293–1307.

Kahsai, A.W., Xiao, K.H., Rajagopal, S., Ahn, S., Shukla, A.K., Sun, J.P., Oas, T.G., and Lefkowitz, R.J. (2011). Multiple ligand-specific conformations of the beta(2)-adrenergic receptor. Nat. Chem. Biol. *7*, 692–700.

Lin, S.Y., Makino, K., Xia, W.Y., Matin, A., Wen, Y., Kwong, K.Y., Bourguignon, L., and Hung, M.C. (2001). Nuclear localization of EGF receptor and its potential new role as a transcription factor. Nat. Cell Biol. *3*, 802–808.

Liu, J.J., Horst, R., Katritch, V., Stevens, R.C., and Wuthrich, K. (2012). Biased signaling pathways in beta(2)-adrenergic receptor characterized by F-19-NMR. Science *335*, 1106–1110.

Lu, C., Mi, L.-Z., Grey, M.J., Zhu, J., Graef, E., Yokoyama, S., and Springer, T.A. (2010). Structural evidence for loose linkage between ligand binding and kinase activation in the epidermal growth factor receptor. Mol. Cell Biol. *30*, 5432–5443.

Luedtke, N.W., Dexter, R.J., Fried, D.B., and Schepartz, A. (2007). Surveying polypeptide and protein domain conformation and association with FlAsH and ReAsH. Nat. Chem. Biol. *3*, 779–784.

Macdonald-Obermann, J.L., and Pike, L.J. (2009). The intracellular juxtamembrane domain of the epidermal growth factor (EGF) receptor is responsible for the allosteric regulation of EGF binding. J. Biol. Chem. *284*, 13570–13576.

Martin-Nieto, J., and Villalobo, A. (1998). The human epidermal growth factor receptor contains a juxtamembrane calmodulin-binding site. Biochemistry *37*, 227–236.

Meier, M., Stetefeld, J., and Burkhard, P. (2010). The many types of interhelical ionic interactions in coiled coils - an overview. J. Struct. Biol. *170*, 192–201.

Nygaard, R., Zou, Y.Z., Dror, R.O., Mildorf, T.J., Arlow, D.H., Manglik, A., Pan, A.C., Liu, C.W., Fung, J.J., Bokoch, M.P., et al. (2013). The dynamic process of beta(2)-adrenergic receptor activation. Cell *152*, 532–542.

Ogiso, H., Ishitani, R., Nureki, O., Fukai, S., Yamanaka, M., Kim, J., Saito, K., Sakamoto, A., Inoue, M., Shirouzu, M., et al. (2002). Crystal structure of the complex of human epidermal growth factor and receptor extracellular domains. Cell *110*, 775–787.

Poppleton, H.M., Sun, H., Mullenix, J.B., Wiepz, G.J., Bertics, P.J., and Patel, T.B. (2000). The juxtamembrane region of the epidermal growth factor receptor is required for phosphorylation of G alpha(s). Arch. Biochem. Biophys. *383*, 309–317.

Reddy, C.C., Wells, A., and Lauffenburger, D.A. (1998). Comparative mitogenic potencies of EGF and TGF alpha and their dependence on receptor-limitation versus ligand-limitation. Med. Biol. Eng. Comput. *36*, 499–507.

Roepstorff, K., Grandal, M.V., Henriksen, L., Knudsen, S.L.J., Lerdrup, M., Grovdal, L., Willumsen, B.M., and van Deurs, B. (2009). Differential effects of EGFR ligands on endocytic sorting of the receptor. Traffic *10*, 1115–1127.

Ryan, S., Verghese, S., Cianciola, N.L., Cotton, C.U., and Carlin, C.R. (2010). Autosomal recessive polycystic kidney disease epithelial cell model reveals multiple basolateral epidermal growth factor receptor sorting pathways. Mol. Biol. Cell *21*, 2732–2745.

Saito, T., Okada, S., Ohshima, K., Yamada, E., Sato, M., Uehara, Y., Shimizu, H., Pessin, J.E., and Mori, M. (2004). Differential activation of epidermal growth factor (EGF) receptor downstream signaling pathways by betacellulin and EGF. Endocrinology *145*, 4232–4243.

Sanders, J.M., Wampole, M.E., Thakur, M.L., and Wickstrom, E. (2013). Molecular determinants of epidermal growth factor binding: a molecular dynamics study. PLoS One *8*, e54136.

Scheck, R.A., and Schepartz, A. (2011). Surveying protein structure and function using bis-arsenical small molecules. Acc. Chem. Res. *44*, 654–665.

Scheck, R.A., Lowder, M.A., Appelbaum, J.S., and Schepartz, A. (2012). Bipartite tetracysteine display reveals allosteric control of ligand-specific EGFR activation. ACS Chem. Biol. *7*, 1367–1376.

Seth, D., Shaw, K., Jazayeri, J., and Leedman, P.J. (1999). Complex post transcriptional regulation of EGF-receptor expression by EGF and TGF-alpha in human prostate cancer cells. Br. J. Cancer *80*, 657–669.

Shaffer, J.P. (1995). Multiple hypothesis-testing. Annu. Rev. Psychol. *46*, 561–584.

Sinclair, J.K., Denton, E.V., and Schepartz, A. (2014). Inhibiting epidermal growth factor receptor at a distance. J. Am. Chem. Soc. *136*, 11232–11235.

Takishima, K., Friedman, B., Fujiki, H., and Rosner, M.R. (1988). Thapsigargin, a novel promoter, phosphorylates the epidermal growth-factor receptor at threonine-669. Biochem. Biophys. Res. Commun. *157*, 740–746.

Thomas, C., Moraga, I., Levin, D., Krutzik, P.O., Podoplelova, Y., Trejo, A., Lee, C., Yarden, G., Vleck, S.E., Glenn, J.S., et al. (2011). Structural linkage between ligand discrimination and receptor activation by type I interferons. Cell *146*, 621–632.

Thoresen, G.H., Guren, T.K., Sandnes, D., Peak, M., Agius, L., and Christoffersen, T. (1998). Response to transforming growth factor or (TGF alpha) and epidermal growth factor (EGF) in hepatocytes: Lower EGF receptor affinity of TGF alpha is associated with more sustained activation of p42/p44 mitogen-activated protein kinase and greater efficacy in stimulation of DNA synthesis. J. Cell Physiol. *175*, 10–18.

Wilson, K.J., Gilmore, J.L., Foley, J., Lemmon, M.A., and Riese, D.J. (2009). Functional selectivity of EGF family peptide growth factors: Implications for cancer. Pharmacol. Ther. *122*, 1–8.

Wilson, K.J., Mill, C., Lambert, S., Buchman, J., Wilson, T.R., Hernandez-Gordillo, V., Gallo, R.M., Ades, L.M.C., Settleman, J., and Riese, D.J. (2012). EGFR ligands exhibit functional differences in models of paracrine and autocrine signaling. Growth Factors *30*, 107–116.

Zhang, X., Gureasko, J., Shen, K., Cole, P.A., and Kuriyan, J. (2006). An allosteric mechanism for activation of the kinase domain of epidermal growth factor receptor. Cell *125*, 1137–1149.

